Published in final edited form as:
Angew Chem Int Ed Engl. 2009 ; 48(23): 4170–4173. doi:10.1002/anie.200805947.

Molecular Photoacoustic Tomography with Colloidal Nanobeacons**

Dipanjan Pan[a,+], **Manojit Pramanik**[b,+], **Angana Senpan**[a], **Xinmai Yang**[b], **Kwang H. Song**[b], **Mike J. Scott**[a], **Huiying Zhang**[a], **Patrick J. Gaffney**[c], **Samuel A. Wickline**[a], **Lihong V Wang**[b], and **Gregory M. Lanza**[a]

Dipanjan Pan: dipanjan@wustl.edu; Lihong V Wang: lhwang@biomed.wustl.edu

[a] C-TRAIN and Division of Cardiology, Washington University School of Medicine, 4320 Forest Park Avenue, Saint Louis, MO 63108, Fax: (+1) 314 454 7490, (Nanobeacons)

[b] Department of Biomedical Engineering, Washington University in St. Louis, One Brookings Drive, St. Louis, MO 63130, Fax: (+1) 314 935 7448, (Photoacoustics)

[c] Department of Surgery St Thomas's Hospital, London, UK

Abstract

Vascularly constrained, "soft" colloidal gold nanobeacons (GNB) demonstrate for the first time that GNBs can be characterized as exogenous photoacoustic contrast agents for targeted detection of fibrin, a major biochemical feature of thrombus. Fibrin-targeted GNBs provide a more than tenfold signal enhancement in photo acoustic tomography (PAT) in the NIR wavelength window, indicating their potential for diagnostic imaging with PAT.

Keywords

Functional Nanobeacons; contrast agents; photoacoustic tomography; molecular imaging; gold; nanoparticles

Molecular imaging has emerged as an interdisciplinary area that shows promise in understanding the components, processes, dynamics, and therapies of a disease at a molecular level.[1–2] The unprecedented potential of nanoplatforms for early detection, diagnosis, and personalized treatment of diseases, is being explored in every noninvasive biomedical imaging modality.[3] Despite myriad advances in the past decade, developing contrast agents with prerequisite features for these imaging modalities continues to remain a challenge.

In the last decade photoacoustic tomography (PAT) has been of particular interest because of its satisfactory spatial resolution and high soft tissue contrast.[4–9] PAT is a novel, hybrid, and nonionizing imaging modality that combine the merits of both optical and ultrasonic imaging methods. It is highly sensitive to the optical absorption of biological tissue. In PAT, tissue is irradiated with a short-pulsed laser beam. Absorption of optical energy causes thermoelastic expansion and radiates photoacoustic (PA) waves from within the irradiated tissue. A wide-band ultrasonic transducer is employed to acquire the PA

**The financial support from the AHA under grant number 0835426N (DP), from NIH under grant numbers NS059302, CA119342 (GML), HL073646 (SAW), U54 CA136398, R01EB000712, R01NS046214, EB008085 (LVW) is greatly appreciated.

Correspondence to: Dipanjan Pan, dipanjan@wustl.edu; Lihong V Wang, lhwang@biomed.wustl.edu.

+These authors contributed equally to this work.

waves, which are then used to quantify the optical absorption distribution in the tissue. Since optical absorption is sensitive to physiological parameters, such as the concentration and oxygenation of hemoglobin, PAT has the potential to provide both functional and molecular imaging *in vivo*. PAT has been used for imaging and quantifying the levels of vascularization and oxygen saturation in tumors.[4–7] These features are associated with angiogenesis and hypoxia accompanying malignant tumors.[10] A number of contrast agents for PAT have been suggested recently,[5,11] but only a few were shown to have the potential for targeted imaging. To achieve molecular PAT, a major and mostly uninvestigated task is to develop nanometric molecular contrast agents. The prerequisite features include improved properties, such as contrast enhancement, stability, and high target specificity.

We have prepared a novel class of accessible and commercially amenable platform technologies: colloidal gold nanobeacons (GNB) of a “soft” nature to target vascular pathology such as thrombus (fibrin), the proximate cause of stroke, and myocardial infarction. Our hypothesis is that GNB will act as an exogenous contrast agent and could be used as a targeted molecular agent in PAT. In a typical synthesis, a commercially available organo-soluble, octylthiol-coated gold nanoparticle (AuNPs, 2 w/v%, 2–4 nm) is suspended in almond oil (20 vol%) and micro fluidized with phospholipid surfactants (2 vol%). The surfactant mixture is comprised of phosphatidylcholine (lecithin-egg PC, 91 mole% of lipid constitutents), cholesterol (8 mole%) and biotin-caproyl-PE (1 mole%). This synthesis resulted in approximately 1200 biotins per nanoparticle for biotin-avidin interaction. A control nanobeacon is prepared identically except for exclusion of the gold nanoparticles.

The GNB particles have a nominal hydrodynamic diameter of 154±10 nm. The polydispersity and zeta potential were measured as 0.08±0.03 and −47±7 mV (Brookhaven Instrument Co.), respectively. Gold content, determined by ICP-MS, was 1080 μg/g of the 20% colloid suspension. UV-Vis spectroscopy confirmed the absorbencies at ~520 nm and in the near-infrared (NIR) window (~900 nm), which correspond to the presence of gold nanobeacons. The particle size and zeta potential of these nanobeacons have varied less than 5% over more than 100 days when stored at 4°C under argon in sealed serum vials (see supporting information). Nanocrystal platforms (<50 nm) for NIR contrast have been reported,[5,11] but particles within this size range rapidly distribute beyond the vasculature and into tissues where binding to non-target cells or simple matrix entrapment can lead to nonspecific signal and increased background noise. For GNB, the tiny metallic gold nanoparticles (2 to 4 nm) are incorporated within a larger, vascular-constrained colloidal particle that is constrained to the circulation and intra-luminal accessible biomarkers.

Figure 2(a) shows the PA signals (λ = 764 nm) obtained from a tygon tube (I.D. 250 μm, O.D. 500 μm) filled with GNB and whole rat blood. At this light excitation the peak-to-peak PA signal amplitude obtained from GNB is ~2.64 V, compared to the ~0.17 V peak-to-peak PA signal amplitude from rat blood. Figure 2(b) shows the PA spectrum (peak-to-peak PA signal amplitude versus excitation light wavelength) of the GNB for an excitation wavelength range of 740–820 nm. The PA spectrum of rat blood is also shown in the same figure. Figure 2(c) plots the ratio of the peak-to-peak PA signal amplitude of GNB to that of rat blood. The PA signal from the tygon tube filled with GNB is more than 15 times strong than that from rat blood. Over the 740–820 nm window the PA signal from GNB is more than ten times stronger. The NIR window is well known for providing deep tissue PA imaging at the expense of blood contrast due to the weak blood absorption. The strong PA signal from GNB in the NIR region indicates the potential for molecular PAT of this platform.

The concept of molecular PAT of fibrin, a critical component of intravascular thromboses, was studied next *in vitro*. Using acellular fibrin clot phantoms, the biotinylated gold nanobeacons and the control nanobeacons (i.e., containing no metal) were targeted to the fibrin clots with classic avidin-biotin interactions using a well-characterized biotinylated anti-human fibrin-specific monoclonal antibody (NIB5F3).[12] Figures 3(a) and 3(b) show cross-sectional PAT images of a LDPE (low density polyethylene) tube (~1 cc volume, I. D. ~6 mm) filled with plasma clot (control) and plasma clot targeted with biotinylated GNB, respectively, using a curved array PAT system.[13] An 800 nm wavelength laser was used for the light source. Both images are shown in the same color bar in Figure 3. The control clot treated with targeted nonmetallic nanoparticles has negligible contrast (Figure 3(a)), whereas the targeted fibrin clot shows up in the PAT image (Figure 3(b)) with high contrast. Figures 3(c) and 3(d) show cross-sectional PAT images, using a PA breast scanner system, [14] of the same control and targeted plasma clot, respectively. For this system, a 532 nm wavelength laser source was used. As expected, the targeted plasma clot is clearly visible (Figure 3(d)) in the PAT image, whereas the control image does not show any plasma clot (Figure 3(c)). We have analytically tested the clot phantoms targeted with three controls, biotinylated-GNB (with gold), non-biotinylated-GNB (with gold) and biotinylated-control nanobeacons (no gold) for total gold content analyses. The total gold content of the clots targeted with biotinylated GNB, non-biotin GNB and biotinylated control nanobeacons (no metal) as determined by ICP-MS, were found to be 47 μg/g, ND (not detected, < 0.02 μg/g) and ND respectively. The *in vitro* images along with ICP-MS data of the targeted plasma clots illustrate the concept of intravascular PAT with GNB.

Preliminary *in vivo* blood vessel imaging was performed non-invasively in a rat model. The pharmacokinetics of GNB in blood vessel following intravenous (IV) injection (3 ml/kg) was monitored from femoral vein as changes in the PA signal with time (Figure 4a). As desirable for molecular imaging, the detection of GNB as a blood pool contrast agent required a 3-fold higher dose IV than would routinely be required for targeted imaging. The expected bi-exponential decay of the PAT signal in blood is similar to reports with other nanoparticles.[1c] Figure 4(b) shows a representative digital photograph of a rat taken prior to imaging with the axillary surface shaved. Figure 4(c) shows the maximum amplitude projection (MAP)[15] photoacoustic image. The vasculature was imaged with high contrast to noise ratio (CNR = 50) and high spatial resolution of ~500 μm. Photoacoustic images were taken immediately after the GNB injection with an interval of 25–30 minutes. Figure 4(d) shows the photoacoustic MAP[15] image (CNR = 68) of the same area 156 minutes after the injection (see supplementary section for details). Both figures 4(c) and 4(d) are shown with the same colorbar. As evident from Figure 4(d), the signal amplitude of the blood vessels was increased by up to ~60% (c and d) compared to that in the control blood vessels, after GNB (0.075 ml) injection.

In summary, we have successfully demonstrated the potential for targeted molecular PAT of GNB as exogenous contrast agents. The gold nanobeacons provide a more than tenfold signal enhancement in PAT in the NIR wavelength window. The *in vitro* and preliminary *in vivo* PAT images both in the NIR wavelength and in the visible wavelength substantiate our hypothesis.

Experimental Section

Preparation of GNB

In a typical experimental procedure, gold nanoparticles (2–4 nm) in toluene (100 mg) are suspended in almond oil (4 mL) and vigorously vortexed to homogeneity. The suspension was filtered through a small bed of cotton. The solvent was evaporated under reduced pressure at 45°C. The surfactant co-mixture included high purity egg yolk

phosphatidylcholine (91 mole%, 377.4 mg), cholesterol (8 mole%, 16.9 mg), and biotinylated-dipalmitoyl phosphatidylethanolamine (1 mole%, 5.8 mg). The surfactant co-mixture is dissolved in chloroform, evaporated under reduced pressure, dried in a 40°C vacuum oven overnight, and dispersed into water by probe sonication. This suspension is combined with the gold nanoparticle-suspended almond oil mixture (20% v/v), distilled de-ionized water (77.3% w/v), and glycerin (1.7%, w/v). The mixture is continuously processed thereafter at 20,000 PSI for 4 minutes with an S110 Microfluidics emulsifier (Microfluidics) at 4°C. The nanobeacons are dialyzed against water using a 20,000 Da MWCO cellulose membrane for a prolonged period of time and then passed through a 0.45 μm Acrodisc Syringe filter. To prevent bacterial growth the nanobeacons are stored under an argon atmosphere typically at 4°C. DLS (D_{av})/nm =154±06 nm; Zeta (ζ)/mV = −47±08 mV; AFM (H_{av})/nm =101±51 nm. (For details, see supporting information)

Photoacoustic Spectroscopy system:[16]

Spectroscopy of the GNB was obtained using this system. Light Source: tunable Ti:sapphire laser (LT-2211A, LOTIS TII) pumped by a Q-switched Nd:YAG (LS-2137/2, LOTIS TII), pulse width: <15 ns, Pulse Repetition Rate (PRR):10-Hz. The incident laser fluence on the sample surface was controlled to conform to the American National Standards Institute (ANSI) standards.[17] Transducer used: 5-MHz central frequency, spherically focused - 2.54 cm focus length, 1.91 cm diameter active area element, and 72% bandwidth (V308, Panametrics-NDT). Amplifier: a low-noise amplifier (5072PR, Panametrics-NDT). Data acquisition: digital oscilloscope (TDS 5054, Tektronix).

Supplementary Material

Refer to Web version on PubMed Central for supplementary material.

References

1. a) Weissleder R, Mahmood U. Radiology. 2001; 219:316. [PubMed: 11323453] b) Whitesides GM. Small. 2005; 1:172–9. [PubMed: 17193427] c) Winter PM, Caruthers SD, Wickline SA, Lanza GM. Nanofabrication towards Biomedical Applications. 2005:227, 49.d) Majoros, IJ.; Baker, JR, Jr. Dendrimer Based Nanomedicine, Edited Book. Pan Stanford Pb; 2008. e) Pan D, Wickline SW, Lanza GM, Caruthers SD. Eur J Radiol. 2009 (online).
2. a) Caruthers SD, Wickline SA, Lanza GM. Curr Opin Biotechnol. 2007; 18:26–30. [PubMed: 17254762] b) Weissleder R, Kelly K, Sun EY, Shtatland T, Josephson L. Nat Biotechnol. 2005; 23:1418. [PubMed: 16244656]
3. a) Hawker CJ, Wooley KL. Science. 2005; 309:1200–5. [PubMed: 16109874] b) O'Reilly RK, Hawker CJ, Wooley KL. Chem Soc Rev. 2006; 35:1068–83. [PubMed: 17057836]
4. Wang XD, Pang YJ, Ku G, Xie XY, Stoica G, Wang LHV. Nat Biotechnol. 2003; 21:803–806. [PubMed: 12808463]
5. Li ML, Oh JT, Xie XY, Ku G, Wang W, Li C, Lungu G, Stoica G, Wang LHV. Proc of the IEEE. 2008; 96:481–489.
6. Wang XD, Xie XY, Ku G, Wang LHV. J Biomed Opt. 2006; 11:024015. [PubMed: 16674205]
7. Lungu GF, Li ML, Xie XY, Wang LHV, Stoica G. Int J Oncol. 2007; 30:45–54. [PubMed: 17143511]
8. Ku G, Wang XD, Stoica G, Wang LHV. Phys Med Biol. 2004; 49:1329–1338. [PubMed: 15128208]
9. Ku G, Wang XD, Xie XY, Stoica G, Wang LHV. Appl Opt. 2005; 44:770–775. [PubMed: 15751858]
10. a) Schneider BP, Miller KD. J Clin Oncol. 2005; 23:1782–1790. [PubMed: 15755986] b) Vaupel P, Mayer A, Briest S, Hockel M. Oxygen Transport to Tissue XXVI. 2005; 566:333–342.
11. a) Agarwal A, Huang SW, O'Donnell M, Day KC, Day M, Kotov N, Ashkenazi S. J Appl Phys. 2007; 102:064701–4. b) Zerda AD, Zavaleta C, Keren S, Vaithilingam S, Bodapati S, Liu Z, Levi

J, Smith BR, Ma T-J, Oralkan O, Cheng Z, Chen X, Dai H, Khuri-Yakub BT, Gambhir SS. Nat Nanotech. 2008; 3:557–562.

12. Raut S, Gaffney PJ. Throm Haemostasos. 1996; 76:56–64.
13. Song KH, Wang LHV. J Biomed Opt. 2007; 12:060503. [PubMed: 18163798]
14. Pramanik M, Ku G, Li CH, Wang LHV. Med Phys. 2008; 35:2218–2223. [PubMed: 18649451]
15. Zhang HF, Maslov K, Stoica G, Wang LHV. Nat Biotechnol. 2006; 24:848–851. [PubMed: 16823374]
16. Song KH, Wang LHV. J Biomed Opt. 2007; 12:060503. [PubMed: 18163798]
17. Laser Institute of America. American National Standard for Safe Use of Lasers ANSI Z136.1-2000. American National Standards Institute, Inc; New York, NY: 2000.

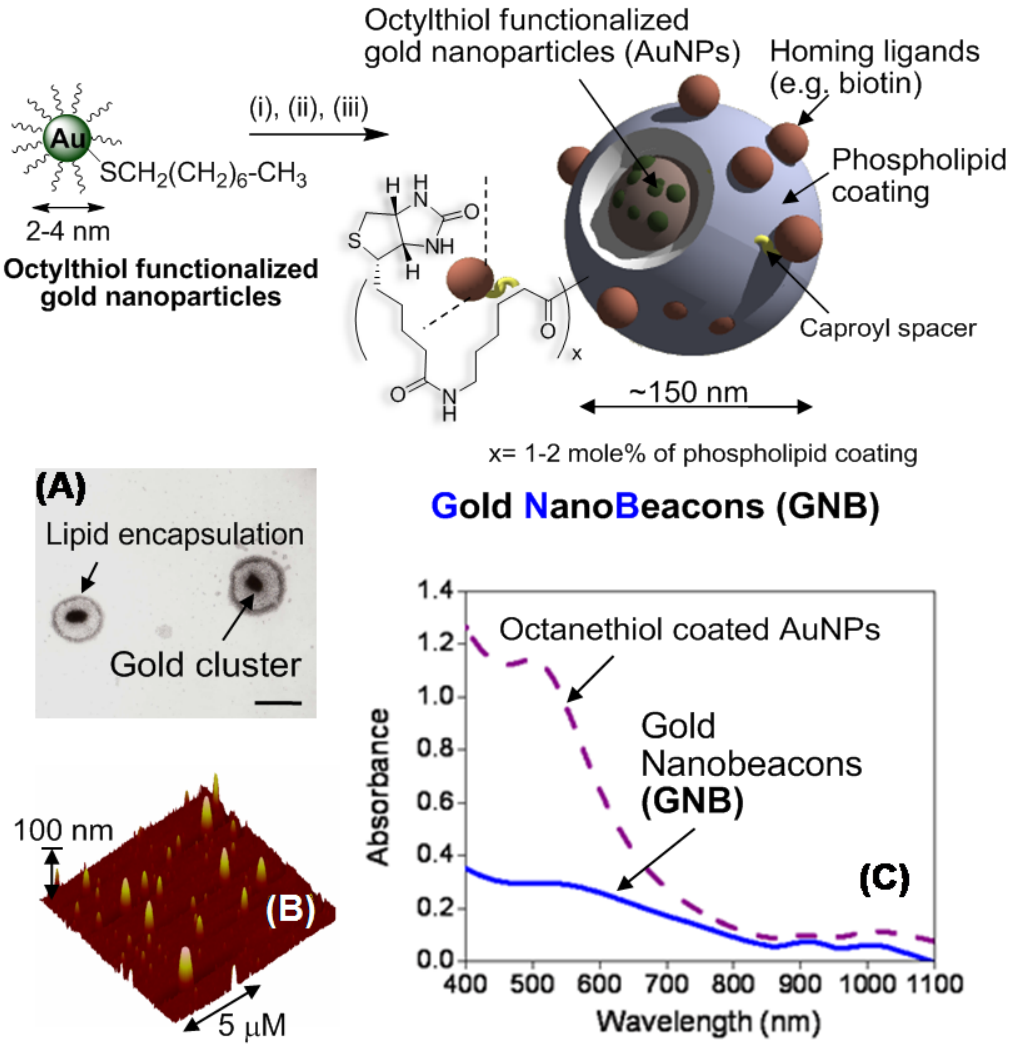

Figure 1.

Preparation of gold nanobeacons: (i) Suspension of octylthiol-coated gold nanoparticle (toluene) in vegetable oil (almond oil), vortex and mixing, filter using cotton bed, evaporation of toluene under reduced pressure at 60°C, vortex; (ii) preparation of phospholipid thin film (iii) resuspension of the thin film in water (0.2 uM), microfludization at 4°C, 12,000 psi, dialysis (cellulosic membrane, MWCO 20K. (A) TEM image of gold nanobeacons (drop deposited over nickel grid, 1% uranyl acetate; scale: 100 nm); (B) AFM image of gold nanobeacons: H_{av}/nm =101±51 nm (C) UV-vis spectroscopic profile (not normalized).

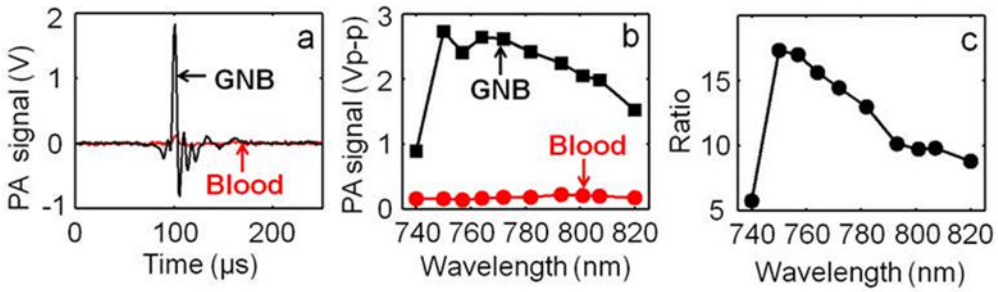

Figure 2.

(a) PA signals generated from a tygon tube (I.D. 250 μm, O.D. 500 μm) filled with GNB and rat blood. The excitation light is of 764 nm wavelength. (b) PA spectrum of GNB and blood over a 740–820 nm range of NIR wavelengths. (c) Ratio of the peak-to-peak PA signal amplitudes generated from GNB to those of blood.

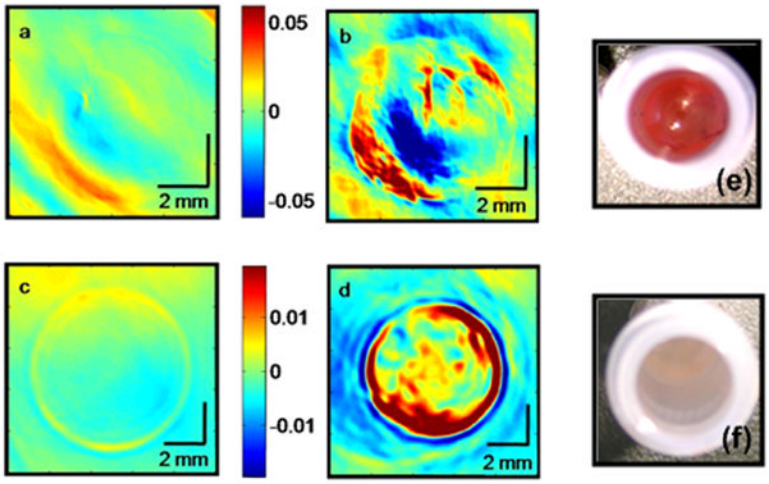

Figure 3.

Cross-sectional PA image of a LDPE tube (~1cc volume, I.D. ~6 mm) filled with plasma clot: (a) control, (b) targeted with GNB using a curved array PA system (λ = 800 nm). (c) Control, (d) targeted with GNB using a photoacoustic breast scanner system (λ = 532 nm). Optical images of plasma clots stained with Biebrich Scarlet-Acid Fuchsin Solution (e) targeted with GNB and (f) control.

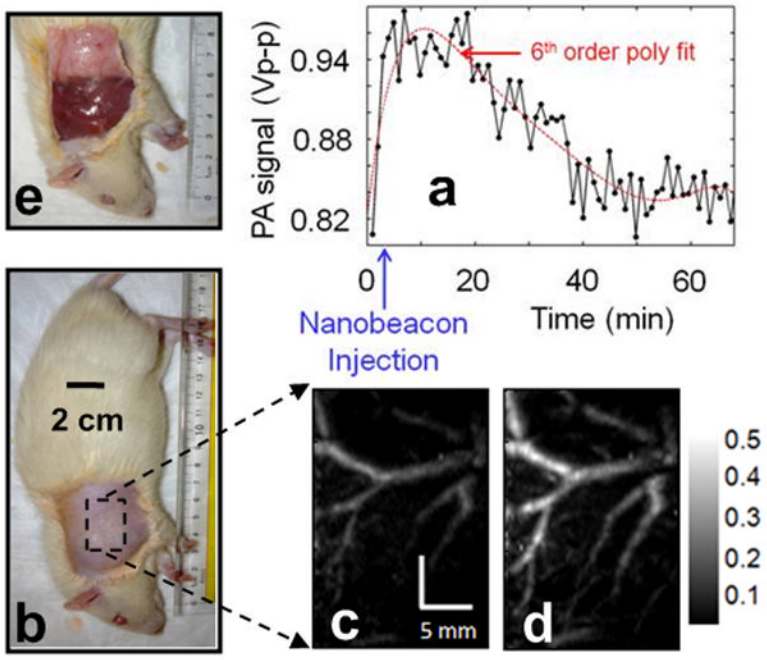

Figure 4.

Non-invasive *in vivo* PA imaging (MAP)[15] of rat. For all PA images, the laser was tuned to 766 nm wavelength. (a) Pharmakokinetics of GNB in blood vessel after injection. The PA signal from the femoral -vein was monitored as intravenous injection (IV) was given with 3 ml/kg doses through tail vein. (b) Photograph of the rat after the hair was removed from the scanning region before taking the PA images. The scanning region is marked with a black dotted square. (c) Control PA image acquired before GNB injection. Bright parts represent optical absorption, here, from blood vessels. (d) PA image (MAP) acquired after 156 minutes of GNB injection (e) Optical photograph of the rat with the skin removed after PA imaging.